nature genetics

Genome-wide association study identifies susceptibility loci for open angle glaucoma at *TMCO1* and *CDKN2B-AS1*

Kathryn P Burdon[1,10], Stuart Macgregor[2,10], Alex W Hewitt[1,3,10], Shiwani Sharma[1], Glyn Chidlow[4], Richard A Mills[1], Patrick Danoy[5], Robert Casson[4], Ananth C Viswanathan[6], Jimmy Z Liu[2], John Landers[1], Anjali K Henders[2], John Wood[4], Emmanuelle Souzeau[1], April Crawford[1], Paul Leo[5], Jie Jin Wang[3,7], Elena Rochtchina[7], Dale R Nyholt[2], Nicholas G Martin[2], Grant W Montgomery[2], Paul Mitchell[7], Matthew A Brown[5], David A Mackey[3,8,9] & Jamie E Craig[1]

We report a genome-wide association study for open-angle glaucoma (OAG) blindness using a discovery cohort of 590 individuals with severe visual field loss (cases) and 3,956 controls. We identified associated loci at *TMCO1* (rs4656461[G] odds ratio (OR) = 1.68, $P = 6.1 \times 10^{-10}$) and *CDKN2B-AS1* (rs4977756[A] OR = 1.50, $P = 4.7 \times 10^{-9}$). We replicated these associations in an independent cohort of cases with advanced OAG (rs4656461 $P = 0.010$; rs4977756 $P = 0.042$) and two additional cohorts of less severe OAG (rs4656461 combined discovery and replication $P = 6.00 \times 10^{-14}$, OR = 1.51, 95% CI 1.35–1.68; rs4977756 combined $P = 1.35 \times 10^{-14}$, OR = 1.39, 95% CI 1.28–1.51). We show retinal expression of genes at both loci in human ocular tissues. We also show that *CDKN2A* and *CDKN2B* are upregulated in the retina of a rat model of glaucoma.

Glaucoma is a group of neurodegenerative ocular diseases united by a clinically characteristic optic neuropathy. It is the second leading cause of blindness worldwide[1]. Primary OAG is the commonest glaucoma subtype[1]. OAG pathogenesis and factors determining disease progression are poorly understood. Early intervention with measures to reduce intraocular pressure retards visual loss in most individuals[2], but many cases of glaucoma remain undiagnosed until after irreversible vision loss. Elucidation of SNPs associated with severe outcomes could enable better targeting of expensive lifelong treatments, with associated morbidity, to individuals with the highest risk of blindness. Linkage and candidate gene studies have identified several genes likely to be involved in OAG including *MYOC* (encoding myocilin)[3] and *NTF4* (ref. 4), although for the latter, findings have varied in different populations[5]. A recent genome-wide association study (GWAS) using Icelandic cases with OAG of unselected severity identified association with variants near *CAV1* (ref. 6). To identify genes predisposing individuals to OAG blindness, we performed a GWAS in Australians of European descent with advanced OAG (individuals with OAG who have progressed to severe visual field loss or blindness).

We selected cases with advanced OAG ($N = 590$ after data cleaning) from the Australian and New Zealand Registry of Advanced Glaucoma (ANZRAG) and the Glaucoma Inheritance Study in Tasmania (GIST)[7,8]. We used two previously described Australian samples as controls ($N = 1,801$ and $N = 2,155$, for a total combined $N = 3,956$)[9]. Cohort demographics are given in **Table 1**, and recruitment and disease definitions are listed in the **Supplementary Note**. We typed samples on Illumina arrays (we typed cases using Omni1 and controls using HumanHap610 or HumanHap660). We combined cases and controls into a single dataset for cleaning and imputation. All participants were Australians of European descent.

After cleaning, 298,778 SNPs were available for association testing. The genomic inflation factor (λ) in the discovery cohort was 1.06 (quantile-quantile plots uncorrected and corrected for λ are shown in **Supplementary Fig. 1a**,**b**). The λ reduced to 1.04 when we included the first ten principal components as covariates. The association results across the genome are displayed in **Figure 1**; results are presented corrected for $\lambda = 1.06$ without correction for principal components. Results with correction for principal components were similar (data not shown). Two regions clearly reached genome-wide significance (defined as $P < 5 \times 10^{-8}$; **Table 2**), with $P = 6.1 \times 10^{-10}$ at rs4656461[G] near *TMCO1* on chromosome 1q24 and $P = 4.7 \times 10^{-9}$ at rs4977756[A] in *CDKN2B-AS1* on chromosome 9p21. Association results at these loci for both genotyped and imputed SNPs are shown in **Figure 2**. Imputation of SNPs from the 1000 Genomes Project did not reveal any SNPs with substantially

[1]Department of Ophthalmology, Flinders University, Flinders Medical Centre, Adelaide, Australia. [2]Genetics and Population Health, Queensland Institute of Medical Research, Brisbane, Australia. [3]Centre for Eye Research Australia, University of Melbourne, Royal Victorian Eye and Ear Hospital, Melbourne, Australia. [4]South Australian Institute of Ophthalmology, Hanson Institute and Adelaide University, Adelaide, South Australia, Australia. [5]The University of Queensland Diamantina Institute, Princess Alexandra Hospital, Brisbane, Australia. [6]Moorfields Eye Hospital, London, UK. [7]Centre for Vision Research, Department of Ophthalmology and Westmead Millennium Institute, University of Sydney, Westmead, Australia. [8]Lions Eye Institute, University of Western Australia, Centre for Ophthalmology and Visual Science, Perth, Australia. [9]Discipline of Medicine, University of Tasmania, Hobart, Australia. [10]These authors contributed equally to this work. Correspondence should be addressed to J.E.C. (jamie.craig@flinders.edu.au).

Received 25 October 2010; accepted 8 April 2011; published online 1 May 2011; doi:10.1038/ng.824

Table 1 Demographic features of the cohorts

	n		Age			% female		
Cohort	Case	Control	Case	Control	*P*	Case	Control	*P*
Discovery	615	3,956	76.6 ± 13.9	43.4 ± 11.5	$<1.0 \times 10^{-6}$	52.1	78.9[a]	$<1.0 \times 10^{-6}$
First replication, advanced glaucoma	334	434	74.9 ± 11.7	78.7 ± 9.1	2.0×10^{-6}	55.6	59.1	0.35
Second replication, less severe glaucoma	465	1,436	71.8 ± 12.6	52.0 ± 0.0	$<1.0 \times 10^{-6}$	61.4	49.7	1.2×10^{-5}
Third replication, Blue Mountains Eye Study	93	2,712	76.5 ± 9.4	70.1 ± 10.1	$<1.0 \times 10^{-6}$	8.5	45.4	$<1.0 \times 10^{-6}$
Combined replication studies	892	4,582	72.0 ± 13.0	64.9 ± 12.4	$<1.0 \times 10^{-6}$	51.1	47.4	0.050

[a]One of the two control cohorts was entirely female, as discussed in the main text.

stronger association than the top genotyped SNPs (**Fig. 2**) or identify additional genome-wide significant loci. At both loci, the most associated SNP is supported by concordant results for other SNPs in moderate or high linkage disequilibrium.

We drew three replication cohorts from the Australian population, and all subjects were of European descent (**Table 1**). The advanced glaucoma replication cohort consisted of 334 additional cases with advanced OAG and 434 controls over 60 years of age (mean age 78.7 years). The less severe cohort consisted of 465 cases with OAG and 1,436 controls from the Wellcome Trust Case Control Cohort 1958 Birth Cohort (WTCCC 58BC). The third cohort was a population-based study, the Blue Mountains Eye Study, containing 93 cases with glaucoma and 2,712 examined controls. The most-associated SNPs at each locus from the discovery cohort clearly replicated in all replication cohorts (**Table 2**). Other SNPs in both of these regions were also associated in the replication cohorts (**Supplementary Table 1a**). Combining all raw data from all replication cohorts in an association analysis gave $P = 7.56 \times 10^{-6}$ (OR = 1.39, 95% CI 1.20–1.61) for rs4656461 near *TMCO1* and $P = 4.19 \times 10^{-7}$ (OR 1.33, 95% CI 1.19–1.48) at rs4977756 in *CDKN2B-AS1* (**Supplementary Table 1b**). These SNPs of interest were also still significantly associated with OAG following adjustments for age and sex in a logistic regression analysis (**Supplementary Table 1b**), indicating that the observed associations are independent of these parameters despite the differences between the case and control cohorts. We combined all available controls to enable a comparison of ORs for the risk alleles at both loci between the advanced OAG cohorts and the less severe OAG cases (**Supplementary Table 1c**). We observed stronger ORs in the advanced cases, and these results support the hypothesis that the risk alleles identified are associated with OAG in general but are more strongly associated with cases which progress to advanced disease. Alternatively, higher diagnostic certainty in severe disease could account for this observation.

Combining raw data from the discovery and all replication cohorts in a study-wide association analysis generated an overall OR = 1.51 (95% CI 1.35–1.68) and $P = 6.0 \times 10^{-14}$ for rs4656461 and OR = 1.39 (95% CI 1.28–1.51) and $P = 1.35 \times 10^{-14}$ for rs4977756 (**Table 2**). Haplotype analyses indicated three common haplotypes around *TMCO1* and two at *CDKN2B-AS1*. The overall *P* values for association were $P = 6.56 \times 10^{-12}$ around *TMCO1* and $P = 2.59 \times 10^{-9}$ at the *CDKN2B-AS1* locus (**Supplementary Table 2**). In both cases, the risk alleles detected in the single SNP analysis are present on a single common haplotype that shows significant association with OAG. The haplotype with the alternative allele at each location appears to be protective against developing OAG. We sequenced 12 individuals with OAG who were homozygous for the risk allele at rs4656461 at all coding exons of *TMCO1* and the 3′ untranslated region (UTR). We found several common SNPs in the 3′ UTR to be present on the risk haplotype, although the functionality of these SNPs is not known (**Supplementary Table 3**). The lack of identified coding variants suggests the true causative variants are likely to be located in a regulatory region of *TMCO1*.

We used two control cohorts in this study; one population sample based on parents of twins and the other a sample of individuals with endometriosis. We subjected cases and controls to the same cleaning regime to ensure a well-matched dataset. The male to female ratio was similar between the case cohort and the twin-based controls, but the endometriosis controls were all female. We repeated the association analysis excluding the endometriosis controls, and this generated *P* values at rs4656461 and rs4977756 of $P = 5.3 \times 10^{-9}$ and $P = 1.1 \times 10^{-7}$, respectively. The reduced significance level of this association can be explained by the smaller sample size, as allele frequencies were very similar between control cohorts (**Supplementary Table 4a**). In addition, we utilized the WTCCC 58BC data as an alternative control cohort for the discovery analysis. The top SNPs at both loci were associated with genome-wide significance levels in this analysis, indicating that our findings do not represent an artifact of the historic controls used (**Supplementary Table 4b** and **Supplementary Fig. 1c**).

To obtain an unbiased estimate of risk for advanced glaucoma, we focused on the first replication cohort[10]. Taking the cases with advanced glaucoma ($N = 334$), the matched examined elderly controls ($N = 434$) and similar age-matched controls from the Blue Mountains Eye Study cohort ($N = 502$), we fitted rs4977756 and rs4656461 into a logistic regression model. Assuming an additive model, individuals carrying four risk alleles (two at each locus) had a 4.50-fold (95% CI 1.84–11.01) higher risk of advanced OAG relative to non-carriers. Grouping individuals with one or two risk alleles together at both loci (dominant model) gave a 3.03-fold (95% CI 1.52–6.07) increased risk. Eighteen percent of the population are in this risk category.

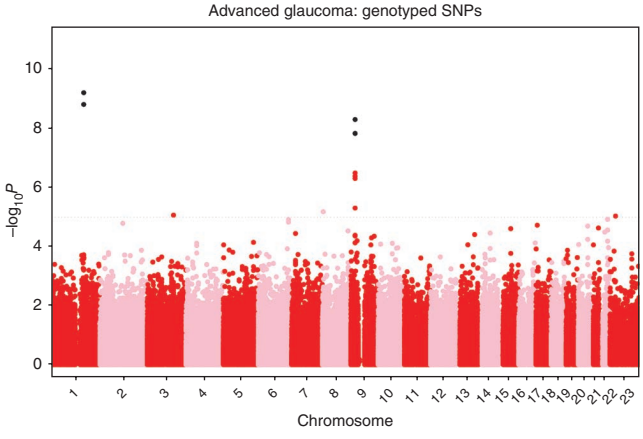

Figure 1 Association results for genotyped SNPs. SNPs with *P* values reaching genome-wide significance ($P < 5 \times 10^{-8}$) are shown in black. Results are corrected for $\lambda = 1.06$. Chromosome 23 refers to the X chromosome.

Table 2 Association results for genome-wide significant genotyped SNPs in the discovery cohort and three replication cohorts and all cases and controls combined (combined studies)

SNP: risk allele	Chr.	Position[a]	Discovery cohort			First replication, advanced glaucoma			Second replication, less severe glaucoma			Third replication, Blue Mountains Eye Study			Combined discovery and replication studies		
			Frequency[b]	*P*[c]	OR (95% CI)	Frequency[b]	*P*	OR (95% CI)	Frequency[b]	*P*	OR (95% CI)	Frequency[b]	*P*	OR (95% CI)	Frequency[b]	*P*	OR (95% CI)
rs4656461:G	1	163,953,829	0.19/0.12	6.1×10^{-10}	1.68 (1.43–1.98)	0.17/0.12	0.010	1.47 (1.09–1.97)	0.15/0.12	0.026	1.28 (1.03–1.59)	0.17/0.12	0.022	1.57 (1.07–2.32)	0.17/0.12	6.0×10^{-14}	1.51 (1.35–1.68)
rs7518099:C	1	164,003,504	0.18/0.12	4.7×10^{-10}	1.67 (1.42–1.96)	0.16/0.12	0.032	1.38 (1.03–1.86)	0.15/0.12	0.022	1.29 (1.04–1.61)	0.18/0.12	0.007	1.68 (1.15–2.46)	0.17/0.12	4.0×10^{-13}	1.49 (1.34–1.66)
rs4977756:A	9	22,058,652	0.69/0.60	4.7×10^{-9}	1.50 (1.31–1.70)	0.69/0.63	0.042	1.25 (1.01–1.56)	0.64/0.58	0.013	1.21 (1.04–1.41)	0.68/0.60	0.015	1.48 (1.08–2.04)	0.67/0.60	1.4×10^{-14}	1.39 (1.28–1.51)
rs10120688:A	9	22,046,499	0.58/0.48	1.4×10^{-8}	1.44 (1.28–1.63)	0.56/0.52	0.153	1.16 (0.95–1.43)	0.51/0.46	0.003	1.27 (1.08–1.48)	0.57/0.48	0.025	1.40 (1.04–1.88)	0.55/0.48	9.1×10^{-12}	1.32 (1.22–1.43)

The frequency of the risk allele in cases and controls is given. All tests were performed under an allelic model.
[a]Position in Build 36. [b]Frequency in cases/controls. [c]Corrected for lambda of 1.06. Chr., chromosome.

Figure 2 Association results for SNPs at the genome-wide significant loci corrected for $\lambda = 1.06$. Genotyped SNPs are indicated by solid triangles, and imputed SNPs are indicated by hollow circles. The top ranked SNP at each locus is shown as a solid diamond. Imputation *P* values for all SNPs are plotted. The color scheme indicates linkage disequilibrium between the top ranked SNP and other SNPs in the region. Note that the imputed and genotyped *P* values for genotyped SNPs differ slightly because for the imputed result, the analysis was based on dosage scores, whereas with genotyped SNPs, the hard genotype calls are used. (**a**) Chromosome 1q24 region. The imputation *P* value was $P = 1.0 \times 10^{-9}$ for the top SNP, rs7524755, with the top genotyped SNP, rs4656461, the fourth best SNP after imputation, with $P = 1.6 \times 10^{-9}$. (**b**) Chromosome 9p21 region. The imputation *P* value was $P = 3.7 \times 10^{-9}$ for the top SNP, rs10757270, with the top genotyped SNP, rs4977756, the second best SNP after imputation, with $P = 8.1 \times 10^{-9}$.

rs4656461 at the 1q24 locus is ~6.5 kb downstream of *TMCO1*. rs4977756 at the 9p21 locus is located within the antisense RNA gene *CDKN2B-AS1*. This region also harbors the tumor suppressor genes *CDKN2A* and *CDKN2B* and is adjacent to *MTAP*. *CDKN2A* also encodes an alternate open reading frame, known as ARF. We analyzed expression of these genes in human ocular tissues by RT-PCR. All the genes are expressed in the iris, ciliary body, retina and optic nerve, but the expression levels varied among the tissues analyzed (**Fig. 3a**). Furthermore, we determined which of the *CDKN2B-AS1* splice variants were expressed in the retina, the tissue that is ultimately compromised in glaucoma. RT-PCR revealed expression of three splice variants of this gene in the human retina (**Fig. 3b**). This is consistent with expression of more than one *CDKN2B-AS1* splice variants in a tissue or cell line[11,12]. We used well-characterized antibodies directed against Cdkn2a, Cdkn2b, Mtap and Tmco1 to explore the distribution of these proteins in rat retina. Cdkn2a and Cdkn2b were expressed in retinal ganglion

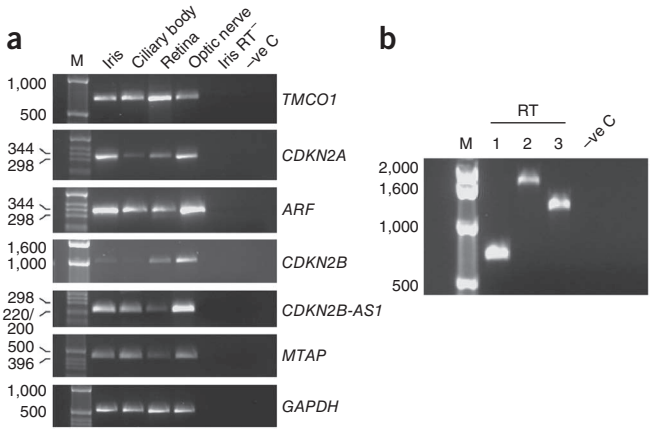

Figure 3 Ocular expression of the genes at the glaucoma-associated loci. (**a**) Analysis of the expression of *TMCO1*, *CDKN2A*/*ARF*, *CDKN2B*, *CDKN2B-AS1* and *MTAP* in various human eye tissues by RT-PCR using gene-specific primers (**Supplementary Table 5**). We amplified *GAPDH* to control for the amount of complementary DNA (cDNA) template used from each tissue for PCR. The expected size of each PCR product is indicated in **Supplementary Table 5**. (**b**) Expression of *CDKN2B-AS1* splice variants in human retina. We performed RT-PCR with gene-specific primers in exon 1 and 19 of *CDKN2B-AS1* (**Supplementary Table 5c**). Lanes 1, 2 and 3 correspond to the splice variants amplified upon primer annealing at 52 °C, 54 °C and 56 °C, respectively. The variant in lane 1 resulted from the splicing of exons 1-5-6-7-19, in lane 2 from the splicing of exons 1-5-6-7-10-11-13-14-15-16-17-18-19 and in lane 3 from the splicing of exons 1-5-6-7-15-16-17-18-19. These variants are different to previously reported *CDKN2B-AS1* variants[11,12]. The full-length variant (DQ485453) and alternatively spliced variants (DQ485454 and GQ495924)[11,12] were undetectable in human retina (data not shown). M, molecular weight markers in base pairs; RT⁻, reverse transcription negative control; –ve C, PCR negative control.

cells (RGC) and other retinal cell types with nuclear patterns of localization, similar to the patterns reported in other tissues (**Supplementary Fig. 2**). Tmco1 was also associated with all retinal cells, but we observed the strongest expression in RGC. Mtap was expressed at low levels in retinal astrocytes (data not shown). To determine whether these genes are candidates for involvement in the pathogenesis of glaucoma, we performed real-time PCR analysis of their expression levels in a validated rat model of glaucoma[13] (**Fig. 4**). We observed strong upregulation of expression of *Cdkn2a* and *Cdkn2b*, but not *Tmco1*, in the retina one week after induction of ocular hypertension, a time point corresponding to ongoing RGC death, as indicated by axonal cytoskeleton damage in the optic nerve of the animals studied.

Recessive mutations in *TMCO1* cause a syndrome consisting of craniofacial dysmorphism, skeletal anomalies and mental retardation[14]. The gene encodes a transmembrane protein with a coiled-coil domain that may localize to the Golgi apparatus and endoplasmic reticulum[15] or to the mitochondria[16] in different cell types. In humans, the gene is ubiquitously expressed in developing and adult tissues[14]. The protein sequence is completely conserved among many mammalian species[14]. Although requiring experimental confirmation, researchers in a previous study proposed a role for TMCO1 in apoptosis[16]. This may suggest a mechanism for the association with glaucoma, which is characterized by excessive RGC apoptosis. It is also possible that other genes adjacent to *TMCO1*, such as *ALDH9A1*, could be responsible for the glaucoma association observed in this study.

CDKN2B-AS1 resides in the 9p21 region that has been clearly associated with cardiovascular disease[17], diabetes[18], intracranial aneurysm[19] and glioma[20]. The antisense RNA encoded by *CDKN2B-AS1* regulates neighboring genes at 9p21, particularly *CDKN2B*, with which its expression levels are reciprocally related[21]. CDKN2B and CDKN2A activate the retinoblastoma tumor suppressor pathway, whereas ARF activates the p53 tumor suppressor pathway. The 9p21 locus is activated in response to oncogenic stimuli[22]. *CAV1*, recently reported to be associated with OAG[6], regulates mitogenic signaling and acts synergistically with *CDKN2A* (ref. 23). Although the *CAV1* SNP (rs4236601) did not reach statistical significance in this GWAS ($P = 0.17$ for a one-sided test), the observed odds ratio of 1.07 is consistent with that previously reported in larger European cohorts, as are the allele frequencies (cases, 0.290; controls, 0.276 for the A allele). It should be noted that many of the cases in the current study are included in the previously reported Australian replication cohort[6]. Genes at the 9p21 locus are known to play a role in aberrant cell division, and we propose that the 9p21 OAG risk variants may predispose RGCs to gradual apoptosis. This hypothesis is supported by observations that the opposite risk alleles in *CDKN2B-AS1* are associated with glaucoma and glioma. For example, at rs4977756 and rs1063192, the G and C alleles, respectively, are protective for glaucoma but are the risk alleles for glioma[20]. The direction of association is the same for glaucoma as for cardiovascular disease[17] and diabetes[18], but further work is required to determine whether the same causative variant(s) underlie these different disease associations.

Recently, rs1063192 in *CDKN2B* was reported to be associated at genome-wide significance with optic cup to disc ratio in healthy individuals[24]. Nominal association of this SNP with glaucoma in a small case series was also reported[24]. In our study, this particular SNP had $P = 3.9 \times 10^{-7}$ in the discovery cohort, and the nearby SNPs in *CDKN2B-AS1* reached genome-wide significance. Thus, we provide further compelling evidence that the 9p21 region is a strong genetic risk factor for OAG in support of the previous suggestive association with OAG at this locus.

This study shows evidence of association of two candidate genes, *TMCO1* and *CDKN2B-AS1*, with advanced OAG, imparting a threefold increase in risk for carriers of one or more risk alleles at the two loci.

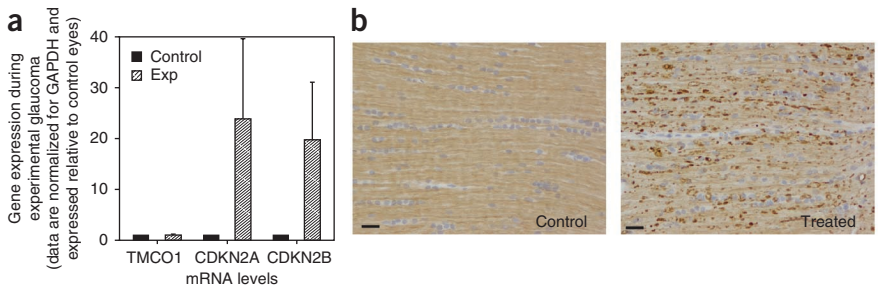

Figure 4 Expression of genes at the glaucoma-associated loci in a rat model of glaucoma. (**a**) Expression of *TMCO1*, *CDKN2A* and *CDKN2B* mRNAs in rat retina 7 days after induction of experimental glaucoma (mean intraocular pressure at time of death of 32 ± 3.7 mm Hg) as determined by quantitative real-time RT-PCR, where $n = 4$. Error bars, s.e.m. (**b**) Axonal degeneration in the distal optic nerve of one representative animal as evaluated by immunolabeling for non-phosphorylated neurofilament heavy protein. Numerous axonal swellings and abnormalities are visible in the optic nerve of the treated eye (right panel) compared with the control optic nerve (left panel), which appears normal. Scale bars in **b**, 25 μm.

In addition, we have shown strong upregulation of *CDKN2A* and *CDKN2B* in response to elevated intraocular pressure, further indicating that this region is important in the molecular pathways leading to glaucoma development. This discovery was made utilizing an approach of selecting cases with severe blinding OAG for the GWAS, but as expected, the risk alleles are also associated with less severe cases, showing the efficacy of using extreme cases to identify genes for a common disease. OAG can be difficult to diagnose in the early stages, and these findings may be useful in the future to prioritize treatment effectively for individuals with possible but not definite early glaucoma (glaucoma suspects), for whom it is often difficult to decide upon the timing of treatment initiation. As treatment for glaucoma is proven to slow disease progression[2], timely initiation of conventional treatment in those individuals at the highest risk could reduce glaucoma blindness. In addition, we have highlighted biochemical pathways involved in this disease, which could lead to more targeted OAG treatment regimes aiming to protect RGC in ways other than lowering intraocular pressure which has until now formed the cornerstone of treatment.

URLs. EIGENSOFT, http://genepath.med.harvard.edu/~reich/Software.htm; MACH2, http://www.sph.umich.edu/csg/abecasis/MACH/index.html; 1000 Genomes, http://www.1000genomes.org; PLINK, http://pngu.mgh.harvard.edu/~purcell/plink/; LocusZoom, http://csg.sph.umich.edu/locuszoom/; Australian & New Zealand Registry of Advanced Glaucoma, www.anzrag.com; European Genome-phenome Archive, http://www.ebi.ac.uk/ega/page.php.

METHODS

Methods and any associated references are available in the online version of the paper at http://www.nature.com/naturegenetics/.

Note: Supplementary information is available on the Nature Genetics website.

ACKNOWLEDGMENTS

This research was funded by the National Health and Medical Research Council (NHMRC) of Australia, project grant 535074 to J.E.C., A.W.H., S.M., D.A.M. and K.P.B. We also thank the following organizations for their financial support: Royal Australian and New Zealand College of Ophthalmologists (RANZCO) Eye Foundation, Clifford Craig Medical Research Trust, Ophthalmic Research Institute of Australia (ORIA), Pfizer Australia, Glaucoma Australia, American Health Assistance Foundation (AHAF), Peggy and Leslie Cranbourne Foundation, Jack Brockhoff Foundation, and National Eye Institute (NEI) Project Grant (2007-2010). The Australian Twin Registry is supported by an NHMRC Enabling Grant (2004-2009). The Queensland Institute of Medical Research (QIMR) Study was also supported by grants from the NHMRC (241944, 339462, 389927, 389875, 389891, 389892, 389938, 443036, 442915, 442981, 496610, 496739, 552485 and 552498), the Cooperative Research Centre for Discovery of Genes for Common Human Diseases, Cerylid Biosciences (Melbourne) and donations from N. and S. Hawkins.

S.M. and K.P.B. are supported by NHMRC Career Development Awards (496674, 613705 and 595944). D.R.N. was supported by the NHMRC Fellowship (339462 and 613674) and Australian Research Council Future Fellowship (FT0991022) schemes. G.W.M., M.A.B. and J.E.C. are supported by the NHMRC Fellowships Scheme. D.A.M. is a recipient of the Pfizer Australia Senior Research Fellowship.

We thank all participants of the Australian and New Zealand Registry of Advanced Glaucoma (ANZRAG), the Glaucoma Inheritance Study in Tasmania (GIST), the Blue Mountains Eye study (BMES), the Queensland Institute of Medical Research (QIMR) study, Oxford Endometriosis Gene Study (OXEGENE), the Nurses Health Study (NHS) and the Brisbane Adolescent Twin Study (BATS) and the staff who have collated clinical data and DNA samples over many years. We thank Glaucoma Australia and Endometriosis Associations for supporting study recruitment. We thank S. Nicolaides, Queensland Medical Laboratory and SA Pathology for *pro bono* collection and delivery of blood samples and other pathology services for assistance with blood collection.

We thank B. Usher, S. Thorpe, A. Kuot, A. McMellon, M. Ring, T. Straga, L. Kearns, J. Barbour, S. Staffieri, J. Ruddle, P. Coleman, M.J. Wright, M.J. Campbell, A. Caracella, L. Bowdler, S. Smith, S. Gordon, K. Zondervan, S. Treloar, J. Painter, B. Haddon, D. Smyth, H. Beeby, O. Zheng and B. Chapman for their input to project management, databases, sample and data collection, sample processing and genotyping. We are grateful to the many research assistants and interviewers for assistance with the studies contributing to the collections used in this project.

We gratefully acknowledge the use of the Wellcome Trust Case Control Consortium 1958 British Birth Cohort data.

AUTHOR CONTRIBUTIONS

K.P.B., S.M., A.W.H., D.A.M. and J.E.C. were involved in the concept and design of this study. A.W.H., R.A.M., R.C., J.L., E.S., J.J.W., N.G.M., G.W.M., P.M., D.A.M. and J.E.C. recruited participants. Genotyping was performed by K.P.B., P.D., A.C.V., A.K.H., J.J.W., D.R.N., N.G.M., G.W.M., M.A.B. and J.E.C. Statistical analysis was undertaken by K.P.B., S.M., J.Z.L., P.L., E.R., D.R.N. and M.A.B. Direct sequencing was performed by K.P.B. and A.C., S.S., G.C., R.C. and J.W. performed the immunohistochemistry and gene expression studies. K.P.B., S.M. and J.E.C. wrote the initial draft. All authors critically revised and provided final approval of this manuscript.

COMPETING FINANCIAL INTERESTS

The authors declare no competing financial interests.

Published online at http://www.nature.com/naturegenetics/.
Reprints and permissions information is available online at http://npg.nature.com/reprintsandpermissions/.

1. Quigley, H.A. & Broman, A.T. The number of people with glaucoma worldwide in 2010 and 2020. *Br. J. Ophthalmol.* **90**, 262–267 (2006).
2. Heijl, A. *et al.* Reduction of intraocular pressure and glaucoma progression: results from the Early Manifest Glaucoma Trial. *Arch. Ophthalmol.* **120**, 1268–1279 (2002).
3. Stone, E.M. *et al.* Identification of a gene that causes primary open angle glaucoma. *Science* **275**, 668–670 (1997).
4. Pasutto, F. *et al.* Heterozygous *NTF4* mutations impairing neurotrophin-4 signaling in patients with primary open-angle glaucoma. *Am. J. Hum. Genet.* **85**, 447–456 (2009).
5. Rao, K.N. *et al.* Variations in *NTF4*, *VAV2*, and *VAV3* genes are not involved with primary open-angle and primary angle-closure glaucomas in an indian population. *Invest. Ophthalmol. Vis. Sci.* **51**, 4937–4941 (2010).
6. Thorleifsson, G. *et al.* Common variants near *CAV1* and *CAV2* are associated with primary open-angle glaucoma. *Nat. Genet.* **42**, 906–909 (2010).
7. Green, C.M. *et al.* How significant is a family history of glaucoma? Experience from the Glaucoma Inheritance Study in Tasmania. *Clin. Experiment. Ophthalmol.* **35**, 793–799 (2007).
8. Hewitt, A.W. *et al.* Sensitivity of confocal laser tomography versus optical coherence tomography in detecting advanced glaucoma. *Clin. Experiment. Ophthalmol.* **37**, 836–841, quiz 903–904 (2009).
9. Painter, J. *et al.* Genome-wide association study identifies a locus at 7p15.2 associated with the development of endometriosis. *Nat. Genet.* **43**, 51–54 (2010).
10. Beavis, W. The power and deceit of QTL experiments: lessons from comparative QTL studies. in *Proceedings of the Corn and Sorghum Industry Research Conference* 250–266 (American Seed Trade Association, Washington, D.C., USA, 1994).
11. Folkersen, L. *et al.* Relationship between CAD risk genotype in the chromosome 9p21 locus and gene expression. Identification of eight new ANRIL splice variants. *PLoS ONE* **4**, e7677 (2009).
12. Pasmant, E. *et al.* Characterization of a germ-line deletion, including the entire *INK4/ARF* locus, in a melanoma-neural system tumor family: identification of ANRIL, an antisense noncoding RNA whose expression coclusters with *ARF*. *Cancer Res.* **67**, 3963–3969 (2007).
13. Ebneter, A., Casson, R.J., Wood, J.P. & Chidlow, G. Microglial activation in the visual pathway in experimental glaucoma: spatiotemporal characterization and correlation with axonal injury. *Invest. Ophthalmol. Vis. Sci.* **51**, 6448–6460 (2010).
14. Xin, B. *et al.* Homozygous frameshift mutation in *TMCO1* causes a syndrome with craniofacial dysmorphism, skeletal anomalies, and mental retardation. *Proc. Natl. Acad. Sci. USA* **107**, 258–263 (2010).
15. Iwamuro, S., Saeki, M. & Kato, S. Multi-ubiquitination of a nascent membrane protein produced in a rabbit reticulocyte lysate. *J. Biochem.* **126**, 48–53 (1999).
16. Zhang, Z. *et al.* Molecular cloning, expression patterns and subcellular localization of porcine *TMCO1* gene. *Mol. Biol. Rep.* **37**, 1611–1618 (2010).
17. Helgadottir, A. *et al.* A common variant on chromosome 9p21 affects the risk of myocardial infarction. *Science* **316**, 1491–1493 (2007).
18. Scott, L.J. *et al.* A genome-wide association study of type 2 diabetes in Finns detects multiple susceptibility variants. *Science* **316**, 1341–1345 (2007).
19. Bilguvar, K. *et al.* Susceptibility loci for intracranial aneurysm in European and Japanese populations. *Nat. Genet.* **40**, 1472–1477 (2008).
20. Shete, S. *et al.* Genome-wide association study identifies five susceptibility loci for glioma. *Nat. Genet.* **41**, 899–904 (2009).
21. Jarinova, O. *et al.* Functional analysis of the chromosome 9p21.3 coronary artery disease risk locus. *Arterioscler. Thromb. Vasc. Biol.* **29**, 1671–1677 (2009).
22. Gonzalez, S. & Serrano, M. A new mechanism of inactivation of the *INK4/ARF* locus. *Cell Cycle* **5**, 1382–1384 (2006).
23. Williams, T.M. *et al.* Combined loss of INK4a and caveolin-1 synergistically enhances cell proliferation and oncogene-induced tumorigenesis: role of INK4a/CAV-1 in mammary epithelial cell hyperplasia. *J. Biol. Chem.* **279**, 24745–24756 (2004).
24. Ramdas, W.D. *et al.* A genome-wide association study of optic disc parameters. *PLoS Genet.* **6**, e1000978 (2010).

ONLINE METHODS

Cohort descriptions. See **Supplementary Note**.

Genotyping and data quality control. Following DNA extraction, Australian twin and endometriosis sample controls were genotyped at deCODE Genetics (Reykjavik, Iceland) on Illumina HumanHap 610W Quad and Illumina Human670Quad Bead arrays, respectively. Cases were genotyped in the laboratory of M.A.B. on Illumina Human1M-Omni arrays. SNPs with a mean BeadStudio GenCall score <0.7 were excluded from the controls. All samples had successful genotypes for >95% of SNPs. SNPs with call rates either <0.95 (minor allele frequency (MAF) > 0.05) or <0.99 (MAF > 0.01), Hardy-Weinberg equilibrium in controls $P < 10^{-6}$ and/or MAF < 0.01 were excluded. Cryptic relatedness was identified through the production of a full identity by state matrix, and 0 cases and 72 controls were removed. Ancestry outliers were identified by principal component (PC) analysis using data from 11 populations of the HapMap 3 and 5 Northern European populations genotyped by the GenomeEUtwin consortium using the EIGENSOFT package[25] and a subset of 160,000 independent SNPs. Individuals (n = 25 cases and 219 controls) lying ≥2 standard deviations from the mean PC1 and PC2 scores were removed. Following these exclusions, there were 590 cases genotyped for 790,038 SNPs and 3,956 controls genotyped for 518,687 SNPs. Our primary analysis was based on a common set of 298,778 SNPs. To investigate population stratification in the cleaned dataset, we generated quantile-quantile plots. These same SNPs were used to generate the first ten principal components for case and control samples combined using EIGENSOFT.

Genomic imputation. Imputation for the Australian twins was performed using MACH2 with data obtained by the Centre d'Etude du Polymorphisme Humain from the 1000 Genomes reference panel 2010_03 release. Imputation was based on a set of autosomal SNPs common to all samples (n = 292,883). The total number of SNPs imputed with imputation $r^2 > 0.5$ was 5,548,553, and these SNPs were taken forward for analysis.

Association analysis. Association analysis was performed using PLINK[26]. Dosage scores from imputation analysis were obtained using MACH2DAT[27]. The analysis was conducted with and without the first ten principal components included as covariates (with negligible difference to results, data not shown). **Figure 2** was prepared using LocusZoom[28].

Replication study genotyping and analysis. All genome-wide significant SNPs were further examined in an independent replication, along with additional SNPs at each locus. SNPs chosen for genotyping were those mapping to each locus defined as within the annotated genes *TMCO1* (four SNPs), *CDKN2A* (two SNPs), *CDKN2B* (two SNPs) or *CDKN2B-AS1* (five SNPS) and ranked within the top 1,000 genotyped SNPs. In addition, SNPs previously reported as associated with other phenotypes at the 9p21 locus but not typed in the discovery phase were also included if the assay design allowed them to multiplex with the other SNPs (four SNPs). SNPs were genotyped using iPLEX Gold chemistry (Sequenom Inc.) in a single plex on an Autoflex Mass Spectrometer (Sequenom Inc.) at the Australian Genome Research Facility (Brisbane, Australia). Genotypes for controls from the BMES cohort were extracted from a previously conducted genome-wide association scan using Illumina HumanHap 670 arrays. Genotypes of the WTCCC 58BC cohort typed on the Illumina HumanHap550 array were downloaded from the European Genome-phenome Archive, and the relevant SNPs were extracted. Each SNP in the replication phase was checked for consistent strand and flipped in one dataset if necessary. The association analysis was conducted in PLINK. Advanced replication cases were compared to 434 elderly examined controls. We compared 465 less severe cases to the WTCCC 58BC data (n = 1,436), and glaucoma cases from within the BMES (n = 93) were analyzed compared to all other participants with available genotype data (n = 2,712). Raw data were pooled for the combined replication cohort analysis and the combined study (discovery and replication cohorts) analysis. An analysis was conducted as for each individual cohort using PLINK. Age and sex were included in a logistic regression analysis under an additive model.

Haplotype analysis. The haplotype analysis was conducted on the combined dataset of all cases, the discovery controls and a subset of BMES controls that were genotyped in house. Analysis was conducted in PLINK. All four *TMCO1* SNPs from the replication phase were included in the haplotype. Prior to analysis, the chromosome 9 locus was assessed in this data for linkage disequilibrium structure using Haploview[29]. The 'solid spine of LD' block definition was used, and this definition identified a block between rs3217992 and rs4977756, and haplotypes were calculated in this block. Inclusion of SNPs outside this block resulted in a large number of rare and less common haplotypes. Only haplotypes with frequency >1% were considered.

Re-sequencing. The coding exons, 3′ UTR and all splice sites of *TMCO1* were sequenced in 12 cases who were homozygous for the risk allele (G) at rs4656461. Primers are given in **Supplementary Table 5**. Each fragment was amplified by PCR with 0.5 U of Hotstart Taq (Qiagen). Following cleanup of PCR products by incubation at 37 °C with 2 U of Shrimp Alkaline Phosphatase (USB) and 10 U of Exonuclease I (New England Biolabs), products were directly sequenced on an ABI PRISM 3100 Genetic Analyzer (Applied Biosystems) with BigDye Terminators (Applied Biosystems) according to standard protocols.

Estimates of effect size in the replication cohort. To calculate an unbiased estimate of risk for advanced glaucoma, we focused on the replication cohort. Taking advanced glaucoma cases (N = 334) and the full set of examined replication controls (N = 936), we fitted rs4977756 and rs4656461 in a logistic regression model using R[30]. Additive effects were modeled by coding SNPs as 0, 1 or 2 risk alleles, and dominance effects were modeled by coding homozygotes as 0 and heterozygotes as 1.

Expression analysis in human ocular tissue. Ocular tissues from postmortem human eyes were obtained through the Eye Bank of South Australia according to guidelines of the Southern Adelaide Health Service/Flinders University Human Research Ethics Committee. Total RNA was extracted using the RNeasy Mini Kit (Qiagen). First strand cDNA was synthesized using the Superscript III reverse transcriptase (Invitrogen) and random hexamers. Human retinal cDNA was synthesized using an oligo-dT primer. PCR was performed using the Hot Star Taq polymerase (Qiagen) and gene-specific primers (**Supplementary Table 5b**). For amplification of *CDKN2B-AS1* splice variants, PCR was performed with gene-specific primer Exon 1F (forward) in combination with either Exon 19R, Exon 12-3′R or Exon 13R primer (reverse) (**Supplementary Table 5c**) in the presence of Q Solution (Qiagen). The specificity of each amplified product was confirmed by sequencing. Coding exons in each variant were determined from alignment with the *CDKN2B-AS1* reference sequence NR_003529.3.

Immunohistochemistry in rat ocular tissue. Tissue sections were deparaffinized in xylene and rinsed in 100% ethanol before treatment with 0.5% H_2O_2 for 30 min to block endogenous peroxidase activity. Antigen retrieval was achieved by microwaving the sections in 10 mM citrate buffer (pH 6.0). Tissue sections were then blocked in 3% normal horse serum made in phosphate buffered saline (PBS), incubated overnight at room temperature (20–25 °C) in primary antibody followed by consecutive incubations with biotinylated secondary antibody (Vector) and streptavidin-peroxidase conjugate (Pierce). Color development was achieved with NovaRED (Vector). Sections were counterstained with hematoxylin, dehydrated and mounted. Specificity of antibody staining was confirmed by incubating adjacent sections with mouse IgG1 isotype control (BD Pharmingen) or normal rabbit serum for the monoclonal antibody and polyclonal rabbit antibodies, respectively. The primary antibodies used were anti-mouse CDKN2A (Abcam, clone 2D9A12, 1:1000), CDKN2B (Cell Signaling Technology, #4822, 1:1000) and anti-rabbit TMCO1 (Aviva Systems Biology, ARP49429_P050, 1:500 to 1:1,000).

For protein blotting to confirm specificity of the TMCO1 antibody, samples from rat liver, brain, retina and optic nerve were sonicated in freshly prepared 20 mM Tris.HCl buffer (pH 7.4) containing 2 mM EDTA, 0.5 mM EGTA, the protease inhibitors phenylmethyl-sulfonyl fluoride (0.1 mM), leupeptin (50 μg/ml) and aprotinin (50 μg/ml) plus a phosphatase inhibitor cocktail. An equal volume of sample buffer (62.5 mM Tris plus HCl, pH 7.4, 4% SDS, 10% glycerol, 10% β-mercaptoethanol and 0.002% bromophenol blue) was added and samples were boiled for 3 min. Samples were size fractionated by SDS-PAGE and transferred onto polyvinylidene fluoride

(PVDF) membrane. The blot was blocked with 5% skimmed milk and Tris buffered saline containing 0.1% Tween 20, probed with antibodies to actin or TMCO1 followed by appropriate secondary antibodies conjugated to biotin and then streptavidin-peroxidase conjugate. The blot was developed with a 0.016% solution of 3-amino-9-ethylcarbazole in 50 mM sodium acetate (pH 5) containing 0.05% Tween-20 and 0.03% H_2O_2.

Evaluation of gene expression levels in a rat model of glaucoma. Sprague-Dawley rats were anesthetized with an intraperitoneal injection of 100 mg/kg ketamine and 10 mg/kg xylazine, and local anesthetic drops were applied to the eye. Ocular hypertension was induced in the right eye of each animal by laser photocoagulation of the trabecular meshwork as previously described[13]. Intraocular pressures were measured in both eyes at baseline, at 8 h and at days 1, 3 and 7 using a rebound tonometer calibrated for use in rats. All rats were killed by transcardial perfusion with physiological saline under deep anesthesia. The retinas were dissected for RT-PCR, and the chiasm from each rat was taken for immunohistochemistry to verify that the procedure had induced an appropriate injury response using the same method detailed above. Total RNA was isolated from each retina, and first strand cDNA was synthesized from 2 μg DNase-treated RNA. Duplicate real-time PCR reactions were carried out using the cDNA equivalent of 20 ng total RNA for each sample in a total volume of 25 μl containing 1× SYBR Green PCR master mix (BioRad) in an IQ5 icycler (Bio-Rad). The primer sets used are detailed in **Supplementary Table 5**. After the final cycle of the PCR, primer specificity was checked by the dissociation (melting) curve method. The relative expression in each sample was calculated using *Gapdh* as reference mRNA as previously described[31].

25. Price, A.L. *et al.* Principal components analysis corrects for stratification in genome-wide association studies. *Nat. Genet.* **38**, 904–909 (2006).
26. Purcell, S. *et al.* PLINK: a tool set for whole-genome association and population-based linkage analyses. *Am. J. Hum. Genet.* **81**, 559–575 (2007).
27. Li, Y., Willer, C., Sanna, S. & Abecasis, G. Genotype imputation. *Annu. Rev. Genomics Hum. Genet.* **10**, 387–406 (2009).
28. Pruim, R. *et al.* LocusZoom: regional visualization of genome-wide association scan results. *Bioinformatics* **26**, 2336–2337 (2010).
29. Barrett, J.C., Fry, B., Maller, J. & Daly, M.J. Haploview: analysis and visualization of LD and haplotype maps. *Bioinformatics* **21**, 263–265 (2005).
30. R Development Core Team. *R: A Language and Environment for Statistical Computing*. (R Foundation for Statistical Computing, Vienna, Austria, 2008).
31. Pfaffl, M.W. A new mathematical model for relative quantification in real-time RT-PCR. *Nucleic Acids Res.* **29**, e45 (2001).

doi:10.1038/ng.824